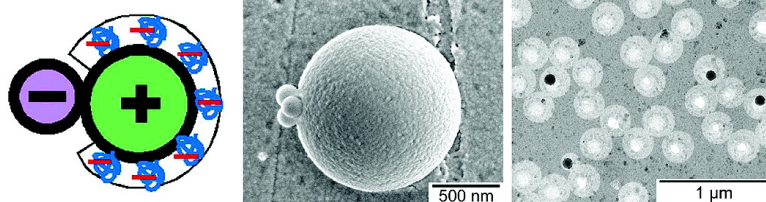


## Preparation and Characterization of Patchy Particles

Thuy T. Chastek, Steven D. Hudson, and Vincent A. Hackley

*Langmuir*, 2008, 24 (24), 13897-13903 • Publication Date (Web): 14 November 2008

Downloaded from <http://pubs.acs.org> on December 11, 2008



### More About This Article

Additional resources and features associated with this article are available within the HTML version:

- Supporting Information
- Access to high resolution figures
- Links to articles and content related to this article
- Copyright permission to reproduce figures and/or text from this article

[View the Full Text HTML](#)



**ACS Publications**  
High quality. High impact.

# Preparation and Characterization of Patchy Particles

Thuy T. Chastek,<sup>\*,†</sup> Steven D. Hudson,<sup>\*,†</sup> and Vincent A. Hackley

National Institute of Standard & Technology (NIST), 100 Bureau Drive,  
Gaithersburg, Maryland 20899-8542

Received June 4, 2008. Revised Manuscript Received October 6, 2008

Anisotropic building blocks are necessary for the self-assembly of complex structures. Methods are reported here for the preparation and characterization of patchy particles. Spherical polymer particles were temporarily bound to a substrate, so that part of their surface is occluded during subsequent surface modification by adsorption of polyelectrolyte. The resulting surface-charge pattern was detected, and its size measured, by means of selective nanoparticle adsorption to this surface. Feasible (roll-to-roll) production rates and process yields are also discussed. In the limit explored here of a single small patch, self-aggregation of patchy particles was observed only at high salt concentration, conditions that suppress anisotropic interactions. Complementary particles however exhibited site-specific binding, to form various anisotropic aggregates.

## Introduction

There has recently been growing interest in using nanoparticles as tailored nanoscale building blocks to be self-assembled into new materials.<sup>1,2</sup> There are several potential advantages to this approach. For example, libraries of nanoparticle building blocks can be prepared and formulated in appropriate compositions to produce materials of interest. Moreover, ongoing success in nanoparticle synthesis has produced new particles with novel shapes and properties such as quantum dots,<sup>3</sup> fluorescently loaded silica particles,<sup>4</sup> gold and silver particles of unique shape,<sup>5</sup> and magnetic nanoparticles.<sup>6</sup> When assembling nanoparticles, a critical consideration is to use particles that are asymmetric either in shape or in chemical composition, otherwise they will only randomly aggregate or assemble onto close-packed lattices. Several strategies for breaking the symmetry of the particles have been described, such as sol–gel polymerization to form dumbbell and triangular shaped particles<sup>7,8</sup> and nanofabricated templates. In template-assisted self-assembly, particles could be linked in a controlled manner through the physical confinement of templated wells and channels.<sup>9,10</sup> This approach has been used successfully to produce a variety of shapes, and microfluidic sorting and shuttling to control such assembly has also been demonstrated.<sup>11</sup> Furthermore, nonspherical particles, such as cube-shaped gold particles, can be prepared directly.<sup>5</sup> Others have produced chemically nonuniform particles with microfluidic flow. Flow streams of monomers are brought together without mixing, and pass through a cross-linking light source. The particles

arise either from using the flow streams to pinch off droplets prior to cross-linking<sup>12,13</sup> or by using a lithographic mask.<sup>14</sup> Other work has created particles using lithographic masks without application of microfluidic flow.<sup>15</sup>

Another method for preparing nonuniform particles is to chemically modify them. This approach can be used easily to modify very small building blocks (e.g., several nanometers), which are difficult to manufacture by top down approaches. The method, sometimes referred to as particle lithography, fundamentally consists of partially coating particles, which are called patchy particles. A great deal of interest in patchy particles has emerged, in part because they can resemble the inhomogeneous surface properties of globular proteins.<sup>16</sup> Zhang and co-workers have simulated the assembly of patchy particles and have predicted several interesting structures,<sup>17,18</sup> such as lattices with diamond symmetry, which have favorable photonic properties. Experimentally, Zhang, et al. have deposited gold vapor onto layers of polystyrene microspheres to coat them with gold nanodots at specific locations.<sup>19</sup> Snyder et al. reported the synthesis of charged polystyrene (PS) patchy particles and formation of anisotropic doublets using particle lithography.<sup>20</sup> Hong et al. prepared charged patchy particles and observed their assembly. The shape of the aggregates observed by epifluorescence microscopy matched predictions based on Monte Carlo simulations.<sup>21</sup> Bianchi et al. reported theoretical and numerical evaluations of the phase diagram of patchy colloidal particles. They observed that the critical point for gas–liquid (or sol–gel) phase separation proceeds to small packing fraction and temperature, with

\* To whom correspondence should be addressed. E-mail: thuy.chastek@nist.gov (T.T.C.); steven.hudson@nist.gov (S.D.H.).

<sup>†</sup> Polymers Division, NIST.

(1) Glotzer, S. C.; Solomon, M. J. *Nat. Mater.* **2007**, *6*, 557–562.  
(2) van Blaaderen, A. *Nature* **2006**, *439*(7076), 545–546.  
(3) Chan, W. C. W.; Maxwell, D. J.; Gao, X. H.; Bailey, R. E.; Han, M. Y.; Nie, S. M. *Curr. Opin. Biotechnol.* **2002**, *13*(1), 40–46.  
(4) Wang, L.; Tan, W. H. *Nano Lett.* **2006**, *6*(1), 84–88.  
(5) Sun, Y. G.; Xia, Y. N. *Science* **2002**, *298*(5601), 2176–2179.  
(6) Sun, S. H.; Zeng, H.; Robinson, D. B.; Raoux, S.; Rice, P. M.; Wang, S. X.; Li, G. X. *J. Am. Chem. Soc.* **2004**, *126*(1), 273–279.  
(7) Johnson, P. M.; van Kats, C. M.; van Blaaderen, A. *Langmuir* **2005**, *21*(24), 11510–11517.  
(8) Kim, J. W.; Larsen, R. J.; Weitz, D. A. *J. Am. Chem. Soc.* **2006**, *128*(44), 14374–14377.  
(9) Yin, Y. D.; Lu, Y.; Gates, B.; Xia, Y. N. *J. Am. Chem. Soc.* **2001**, *123*(36), 8718–8729.  
(10) Yin, Y.; Lu, Y.; Xia, Y. *J. Am. Chem. Soc.* **2001**, *123*, 771–772.  
(11) Sung, K. E.; Vanapalli, S. A.; Mukhija, D.; McKay, H. A.; Millunchick, J. M.; Burns, M. A.; Solomon, M. J. *J. Am. Chem. Soc.* **2008**, *130*(4), 1335–1340.

(12) Nie, Z. H.; Li, W.; Seo, M.; Xu, S. Q.; Kumacheva, E. *J. Am. Chem. Soc.* **2006**, *128*(29), 9408–9412.

(13) Shepherd, R. F.; Conrad, J. C.; Rhodes, S. K.; Link, D. R.; Marquez, M.; Weitz, D. A.; Lewis, J. A. *Langmuir* **2006**, *22*(21), 8618–8622.

(14) Dendukuri, D.; Pregibon, D. C.; Collins, J.; Hatton, T. A.; Doyle, P. S. *Nat. Mater.* **2006**, *5*(5), 365–369.

(15) Hernandez, C. J.; Mason, T. G. *J. Phys. Chem. C* **2007**, *111*(12), 4477–4480.

(16) Glotzer, S. C. *Science* **2004**, *306*(5695), 419–420.

(17) Zhang, Z. L.; Keys, A. S.; Chen, T.; Glotzer, S. C. *Langmuir* **2005**, *21*(25), 11547–11551.

(18) Zhang, Z. L.; Glotzer, S. C. *Nano Lett.* **2004**, *4*(8), 1407–1413.  
(19) Zhang, G.; Wang, D. Y.; Mohwald, H. *Angew. Chem., Int. Ed.* **2005**, *44*(47), 7767–7770.

(20) Snyder, C. E.; Yake, A. M.; Feick, J. D.; Velegol, D. *Langmuir* **2005**, *21*, 4813–4815.

(21) Hong, L.; Cacciuto, A.; Luijten, E.; Granick, S. *Nano Lett.* **2006**, *6*(11), 2510–2514.

decreasing number of patchy sites.<sup>22</sup> For mixtures of particles having either two or three patchy sites, the liquid (network) phase is stable to very small packing fraction. In addition, they calculated cluster size distributions.<sup>23</sup> They confirmed that the patchiness has a strong effect on the phase diagram for both ordered and disordered arrangements of the sites on the hard sphere surface.<sup>24</sup>

A limitation associated with previous experimental work has been the difficulty to produce large numbers of coated particles. A primary challenge to increasing yield is to create unaggregated particle monolayers with high coverage, for subsequent use in coating. Deposition of particles onto a bare glass substrate results in either a low degree of coverage (which causes slow production rates) or aggregation in the dried state. Any aggregation in this initial step ultimately reduces the uniformity in the final self-assembled product, thereby reducing the applicability of the materials. This paper explores the use of a polyelectrolyte-coated substrate to improve this initial step, and it characterizes the particle lithography process structurally, and in terms of throughput and yield. It also reports the assembly behavior of these patchy particles, both self-aggregation and site-specific binding of complementary particles.

### Experimental Section

**Materials.** All chemicals were used as received: anionic polyelectrolyte poly(sodium 4-styrene sulfonate) (PSS, number-average molar mass  $M_n \approx 70\,000$  g/mol, 30% by mass in water, from Aldrich<sup>25</sup>), cationic polyelectrolyte poly(allylamine hydrochloride) (PAH,  $M_n \approx 70\,000$  g/mol, Aldrich), potassium hydroxide (KOH, Aldrich), ethanol (200 proof, Warner-Graham Co.), and sodium chloride (NaCl, J.T. Baker). The radii of gyration for the two polyelectrolytes are approximately 31 nm (PSS in 0.5 mol/L NaCl)<sup>26</sup> and 22 nm (PAH in 0.05 mol/L NaCl).<sup>27</sup> These radii decrease somewhat at elevated salt concentration. The following polymer concentrations were prepared and used: a.) 4.1 mg/mL PSS and b.) 1.87 mg/mL PAH, each in 2.0 mol/L NaCl. The polyelectrolyte concentrations are near the overlap concentration.

Polystyrene (PS) spheres ranging from 40 to 4690 nm in diameter were purchased from Invitrogen and from Polysciences. Additional polystyrene particles (600 nm diameter) were prepared using a previously reported emulsion polymerization method.<sup>28,29</sup> Distilled and deionized (DI) water (Millipore, specific resistance = 18  $M\Omega \cdot \text{cm}$ ) was used for all experiments and washing steps. In this report, we employ a systematic nomenclature for particles and their surface coating. For example, PS600s<sup>-</sup> denotes a polystyrene particle, diameter 600 nm, sulfate surface chemistry, with negative surface charge. PS600s<sup>(-)+</sup> and PS600s<sup>(-)+</sup> denote the same particle coated with the cationic polyelectrolyte, either completely or on only part of its surface, respectively.

**Preparatory Methods.** Patchy particles were prepared by particle lithography, involving the following sequential steps: substrate preparation, particle adsorption, surface treatment, and particle detachment. Briefly, a glass slide was cleaned in a base bath with

(22) Bianchi, E.; Largo, J.; Tartaglia, P.; Zaccarelli, E.; Sciortino, F. *Phys. Rev. Lett.* **2006**, *97*(16), 168301.

(23) Bianchi, E.; Tartaglia, P.; La Nave, E.; Sciortino, F. *J. Phys. Chem. B* **2007**, *111*, 11765–11769.

(24) Bianchi, E.; Tartaglia, P.; Zaccarelli, E.; Sciortino, F. *J. Chem. Phys.* **2008**, *128*, 144504-1–144504-10.

(25) Equipment and instruments or materials are identified in the paper in order to adequately specify the experimental details. Such identification does not imply recommendation by NIST, nor does it imply the materials are necessarily the best available for the purpose.

(26) Prabhu, V. M.; Muthukumar, M.; Wignall, G. D.; Melnichenko, Y. B. *J. Chem. Phys.* **2003**, *119*(7), 4085–4098.

(27) Burchard, W.; Frank, M.; Michel, E. *Ber. Bunsen-Ges.* **1996**, *100*(6), 807–814.

(28) Schrodin, R. C.; Al-Daous, M.; Sokolov, S.; Melde, B. J.; Lytle, J. C.; Stein, A.; Carbajo, M. C.; Fernandez, J. T.; Rodriguez, E. E. *Mater. Chem.* **2002**, *12*, 3261–3327.

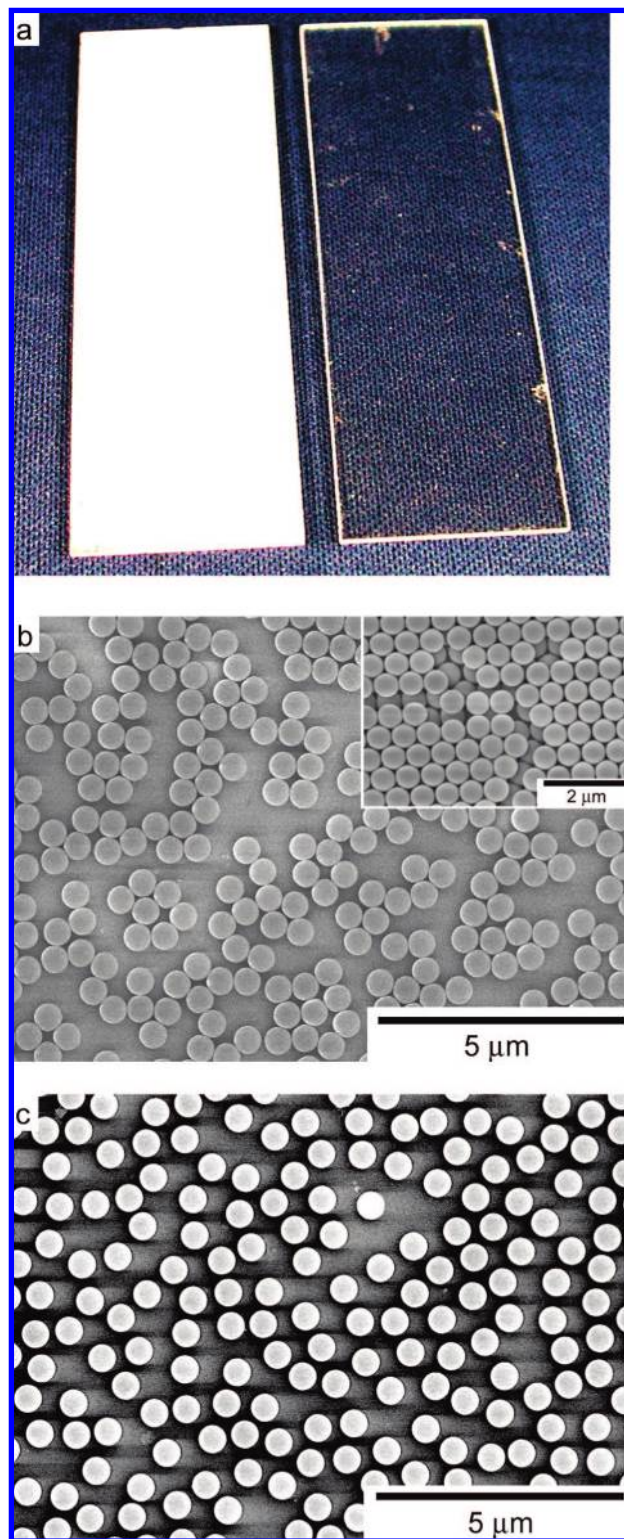


**Figure 1.** Monolayers of PS600s<sup>-</sup> particles. (a) Photographs of glass slides with PS600s<sup>-</sup> particles absorbed during 1 min onto a polyelectrolyte multilayer (left) having higher particle density and yield than the same particles adsorbed onto a bare glass for 48 h (right). (b) SEM image of PS600s<sup>-</sup> particles adsorbed (5 min) onto a polyelectrolyte multilayer and then dried. Inset: close packed structure produced by flow coating. (c) As in (b), yet heated to 80 °C for 60 s before drying.

1% mass KOH in a mixture of water/ethanol (3:7) and dried under N<sub>2</sub>(g). Multilayer polyelectrolyte assemblies were prepared by consecutive alternating adsorption of cationic and anionic polyelectrolyte layers from 2.0 mol/L NaCl solutions, as noted above.

**Table 1. Zeta Potentials (mV) of Polystyrene Particles of Various Size and Charge**

particle <sup>a</sup>	$\zeta$ (mV)
PS1200a <sup>+</sup>	7.4 ± 0.7
PS1200a <sup>+-</sup> (0.3 mol/L NaCl)	-32.5 ± 2.3
PS1200a <sup>+-</sup> (0.1 mol/L NaCl)	-55.1 ± 3.8
PS600s <sup>-</sup>	-34.3 ± 0.5
PS600s <sup>-+</sup> (0.3 mol/L NaCl)	38.0 ± 1.4
PS160c <sup>-</sup>	-32.9

<sup>a</sup> See text for particle nomenclature. As-received surface chemistry is denoted as a (amidine), s (sulfate), or c (carboxyl). Standard uncertainties of the measured zeta potential are reported.

The traditional polyelectrolyte coating procedure is dipping successively into polyelectrolyte solutions and in water rinse baths,<sup>30,31</sup> and typically several minutes is required for equilibrium coating at each step.<sup>32</sup> A much faster spraying process has also been developed.<sup>33,34</sup> In this process, the substrate is sprayed repeatedly with polyelectrolyte solutions and water rinse, which drain over the surface (held vertically). Hydrodynamic effects associated with this drainage have been suggested to increase mass transfer and adsorption rates. The polyelectrolyte layer reaches its final saturated state asymptotically after approximately six spray applications of solution and rinse. At approximately 12 s/cycle of solution and rinse, saturated layers may be produced in approximately 1 min.

Here, we use a different rapid coating technique, with comparable speed, that uses polyelectrolyte solution much more efficiently and mimics an efficient roll-to-roll process. (Since the vast majority of the solution drains away during spray coating, it is either wasted or must be collected.) In our technique, the substrate to be coated is placed briefly (1 s) in contact with the polyelectrolyte solution; it is then held upright (vertical), with its edge touching the solution, so that surface tension removes the excess bead of solution that would otherwise hang from the substrate (holding again approximately 1 s). By switching alternately between these two positions, 10 cycles are accomplished in 20 s. Washing is done likewise, by contacting the face and edge of the substrate onto clean water, to remove excess polyelectrolyte. In this way, multilayers can be built up rapidly (e.g., 80 s/bilayer). We have not carried out ellipsometry or reflectivity on these multilayer films to evaluate their structure, but they behave similarly in particle adsorption experiments to those films prepared by standard slow dip-coating procedures.

Typically, 3 or 3.5 bilayers were deposited onto clean glass, so that the outermost layer was either PSS or PAH, respectively. These dried films were then exposed to a particle suspension for 1–5 min to prepare an unaggregated particle monolayer.<sup>35,36</sup> Substrates were selected so to have a charge opposite to that of the particles. The monolayer of particles was washed thoroughly with DI water.

Without drying, this assembly was then coated with a polyelectrolyte film, under standard and rapid dipping conditions as described above. The polyelectrolyte may adsorb everywhere (on substrate and particle) except where the two surfaces (particle and substrate) occlude one another and the polyelectrolyte is size-excluded. After such adsorption, the sample was washed repeatedly with DI water to remove any excess polyelectrolyte and then placed in 10 mL of a NaCl solution (0.1–5.0 mol/L, aq) and sonicated to detach adsorbed PS particles from the glass slide. The resulting particles were

concentrated by removing salt solution with a Millipore stirring cell (0.2–0.6  $\mu\text{m}$  pore size) until the final volume was approximately 2.0 mL.

Assemblies of particles were prepared by mixing the patchy PS particle solutions with a drop of appropriately charged particles and stirring for at least 10 h. When assembling large patchy particles with small uniform particles, the solution was filtered using an ultrafiltration Millipore stirred cell with appropriate pore size to remove the small particles that had not attached to the patchy particles. The solution was washed repeatedly with a NaCl solution (0.1–0.3 mol/L) to further remove nonadsorbed particles.

**Characterization Methods.** The steps just described were monitored *in situ* by optical microscopy in bright field, using an Olympus IX71 inverted optical microscope, with either a 20 $\times$  (NA = 0.4) or a 60 $\times$  water-immersion (NA = 1.2) objective lens and with a charge-coupled device (CCD) camera. These observations were used to determine if any of the process steps (and variations of them) caused particles to move or detach prematurely. Fiducial marks and shadow evaporation (discussed below) facilitated these measurements. In addition, particle and aggregate suspensions were also examined by optical microscopy.

Slight variations of the preparatory methods described above were used to characterize these processes. The following is the method used to characterize the size-excluded polyelectrolyte adsorption process, whereby either the particles or the substrate may be patterned, that is, partially coated with polyelectrolyte. A dry particle monolayer (touching spheres ok) was first coated with chromium by vacuum evaporation, so that each particle casts a shadow nearly vertically toward the substrate, thus marking its position. The sample was then rapidly dip-coated in polyelectrolyte solution and then washed in DI water. To produce a charged pattern on the substrate, the polyelectrolyte here was of the same sign as the surface charge of the particle. When a thicker film was desired to enable mass-thickness contrast examination by transmission electron microscopy (TEM), polyelectrolyte multilayers were deposited. Nearly all of the particles remained in position, as verified by optical microscopy. The particles were then removed by sonication and washing. To demarcate the resulting surface-charge pattern on the substrate, this substrate was exposed to a suspension of charged fluorescent polystyrene nanoparticles for 10–300 min, washed with DI water, and dried with N<sub>2</sub>(g). (Various sizes of nanoparticles were used depending on requirements for fluorescence brightness and size relative to patch.) In some instances, this surface was also shadowed with Pt/C by vacuum evaporation to enhance contrast of topography. Finally, the surface was coated with evaporated carbon. The accumulated coatings (schematically shown in Figure 2a) were then removed from the substrate using poly(acrylic acid) (PAA). An aqueous solution of PAA was cast on the surface in contact with the top layer of carbon and allowed to dry. The resulting glassy polymer chip was removed, bringing the underlying coatings with it. Floating this chip (coating side up) onto the surface of distilled water, the PAA was washed away and the coatings retrieved on copper grids. The specimens were then examined by bright-field TEM, using a Philips EM 400T microscope operated at 120 kV.

Particles and their assemblies were also analyzed by scanning electron microscopy (SEM) using a Hitachi S 4700 microscope. Samples were prepared by depositing particles onto polyelectrolyte-coated glass slides and sputtering thin layers of gold at 13.3 Pa, 45 mA, and 90 s.

The average zeta potential ( $\zeta$ ) of the particles (based on at least 10 independent measurements) was determined at 20 °C using a Zetasizer 3000HS instrument (Malvern Instruments, Southborough, MA). This instrument measures the electrophoretic mobility in a quartz capillary using laser Doppler velocimetry. The zeta potential was also measured with a Zeta-Reader instrument (Zeta Potential instruments, Bedminster, NJ), which uses direct imaging (i.e., particle tracking) to measure electrophoretic mobility.<sup>37</sup>

(29) Wang, Z.; Ergang, N. S.; Al-Daous, M. A.; Stein, A. *Chem. Mater.* **2005**, *17*, 6805–6813.

(30) Decher, G.; Hong, J. D.; Schmitt, J. *Thin Solid Films* **1992**, *210*(1–2), 831–835.

(31) Decher, G. *Science* **1997**, *277*(5330), 1232–1237.

(32) Bertrand, P.; Jonas, A.; Laschewsky, A.; Legras, R. *Macromol. Rapid Commun.* **2000**, *21*(7), 319–348.

(33) Schlenoff, J. B.; Dubas, S. T.; Farhat, T. *Langmuir* **2000**, *16*(26), 9968–9969.

(34) Izquierdo, A.; Ono, S. S.; Voegel, J. C.; Schaaff, P.; Decher, G. *Langmuir* **2005**, *21*(16), 7558–7567.

(35) Serizawa, T.; Takeshita, H.; Akashi, M. *Langmuir* **1998**, *14*, 4088–4094.

(36) Serizawa, T.; Takeshita, H.; Akashi, M. *Chem. Lett.* **1998**, 487–488.

(37) The standard uncertainty of this measurement is approximately 5%.

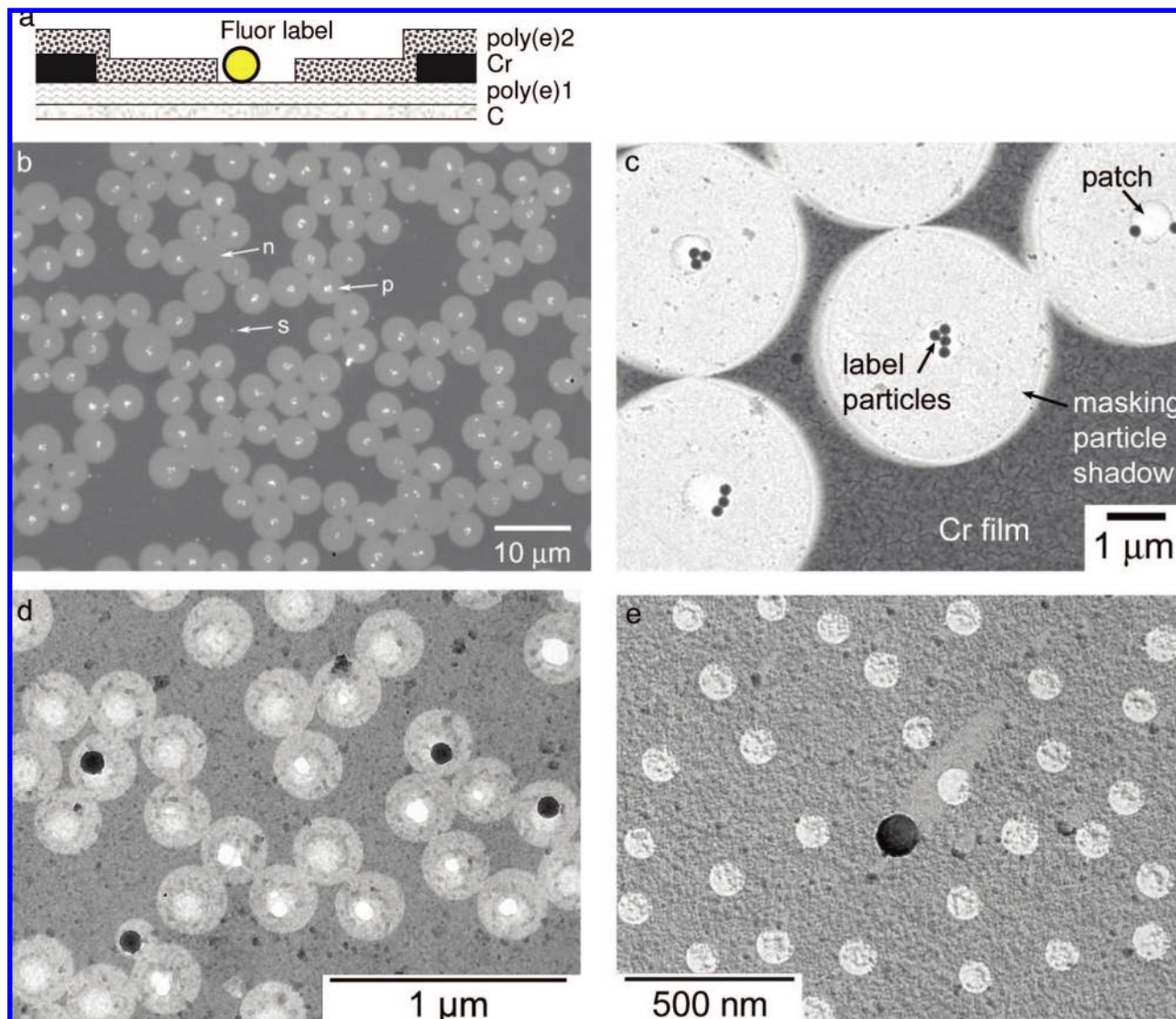


**Figure 2.** Images of accumulated layers, following processes to produce and reveal surface-charge patterns on the substrate. (a) Schematic of accumulated layers. (b) Fluorescence microscopy (with bright-field backlight). The dark background is an evaporated Cr layer that marks out the location of the PS4690s<sup>-</sup> masking spheres (gray). Patch sites (e.g., labeled “p”) are labeled with bright fluorescent PS100s<sup>-</sup> particles. A stray fluorescent particle is labeled “s”. The location labeled “n” is one of two types of sites (see text) without PS100s<sup>-</sup> particles. (c) TEM image of a sample, as in (b), yet with PS200s<sup>-</sup> spheres adsorbed to positively charged patches, visible by mass-thickness contrast. (d) TEM image with PS300s<sup>-</sup> as the masking spheres. Four PS100s<sup>-</sup> particles (dark) are adsorbed to different positively charged patch sites. (e) TEM image with PS100s<sup>-</sup> as the masking spheres. Circular patches within the light gray circles are barely visible by mass-thickness contrast.

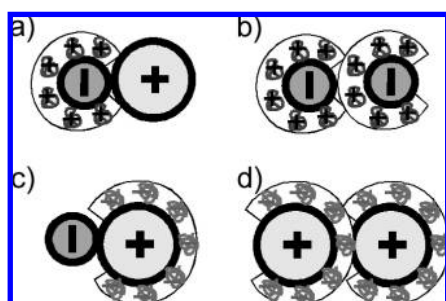


**Figure 3.** Schematic of possible doublet types: (a) A<sup>-</sup>+B<sup>+</sup>, (b) A<sup>-</sup>+A<sup>-</sup>+, (c) A<sup>-</sup> B<sup>+</sup>+, and (d) B<sup>+</sup>+ B<sup>+</sup>+

### Results and Discussion

**Particle Monolayers.** As noted above, the process to produce patchy particles involves the formation of particle monolayers. Both negatively and positively charged PS particles were used in this study, and their  $\zeta$  values are listed in Table 1. These PS

particles were adsorbed onto oppositely charged (cationic or anionic) substrates by electrostatic interactions, which increased and accelerated adsorption. A large degree of surface coverage was attained after 1–5 min (Figure 1). In contrast, Snyder et al.<sup>20</sup> and Hong et al.<sup>21</sup> deposited particles onto bare glass substrates and found that deposition onto those substrates is much slower (e.g., ~24 h). This sluggishness is a more pronounced problem for negatively charged particles given the slight negative charge of glass. For example, for a single concentration (0.5% mass in water), PS600s<sup>-</sup> particles deposited uniformly to cover the entire surface of a glass slide coated with positively charged poly-electrolyte, whereas few particles were coated onto the bare glass substrate. Figure 1a shows the degree of particle adsorption is visibly apparent, differing by approximately 1 order of magnitude between the two procedures. Moreover, the coverage of particles on bare glass is extremely low in the wet state, and when dried the particles are drawn together by capillary forces.<sup>38</sup> Indeed,

(38) Hanarp, P.; Sutherland, D. S.; Gold, J.; Kasemo, B. *Colloids Surf., A* **2003**, *214*(1–3), 23–36.

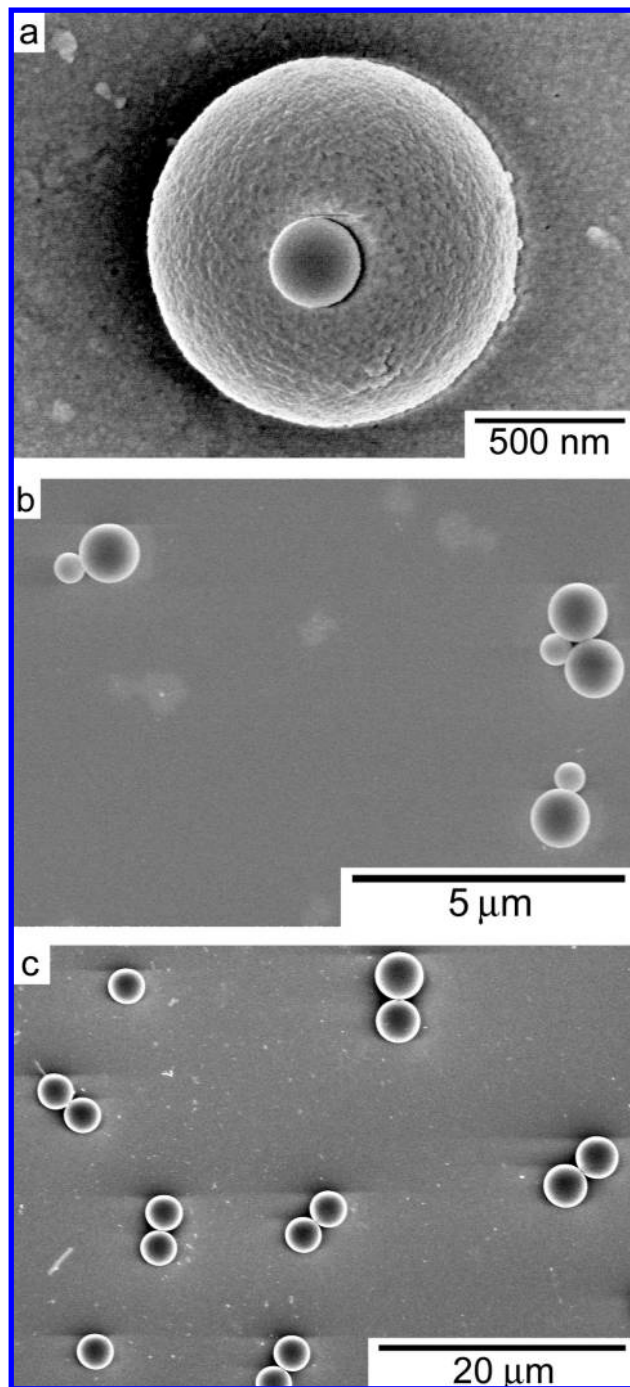


**Figure 4.** SEM micrographs of doublet formation: (a) PS1200a<sup>+</sup>/PS300c<sup>-</sup>; (b) PS1200a<sup>+</sup>/PS600s<sup>-</sup>; and (c) (PS3200a<sup>+</sup>)<sub>2</sub>.

these forces can be used to produce large-area close-packed monolayers.<sup>39</sup> These capillary forces scale with particle size, so that the aggregation of particles may be observed even on polyelectrolyte films if the particle diameter exceeds 500 nm. This aggregation process was observed in real-time by bright-field optical microscopy, and the resulting particle clusters were observed by SEM (Figure 1b).

Several routes to circumvent this surface-tension-driven aggregation during drying were examined. These included methods to increase particle adhesion to the substrate (by waiting or heating) or reduce surface tension. Surface tension can be

reduced by replacing the surrounding liquid. Attempts were made therefore to wash samples with ethanol, prior to drying, but this reduction in surface tension was insufficient to prevent aggregation. Critical point drying undoubtedly would be sufficient, but was not attempted. On the other hand, mild heat treatment or waiting time was sufficient to adhere particles to the polyelectrolyte substrate,<sup>40</sup> thereby preventing aggregation during drying. Samples were treated in a hot DI water bath at different temperatures and heating times. Noncontacting particles were observed in the dry state by SEM for the samples heated to 80 °C for 60 s (Figure 1c); 2 min at 60 °C was also sufficient. These conditions are well below the glass transition temperature of polystyrene, and the particles show no evidence of distortion.

During typical preparations in this work, the films and particle monolayers were maintained in the wet state throughout, eliminating the need for heating or waiting. This route to unaggregated monolayers is expected to simplify production of patchy particles in many situations, and applicability to roll-to-roll processes is likely.

**Patchy Surfaces.** As noted above, surface-charge patterns on either the substrate (Figure 2) or the particles result from coating the particle monolayer with a polyelectrolyte that has either the same or opposite charge as the particles, respectively. This polyelectrolyte is excluded from the contact region, as determined by the blob size of the polyelectrolyte<sup>41</sup> (diameter  $d_b$ ) and the curvature of the spherical particle (radius  $a$ ). The radius of the excluded (lithographic) region is calculated geometrically to be approximately<sup>20</sup>

$$r_{\text{patch}} = (ad_b)^{1/2} \quad (1)$$

After adsorption of the polyelectrolyte, the masking spheres are removed from the substrate by sonication. The time of sonication required to remove the particles increases with decreasing particle size and increasing waiting time, as expected.<sup>40,42,43</sup> Particle lithography was carried out for a variety of masking particle sizes, ranging from 4690 to 100 nm (Figure 2). Correspondingly, sonication time was varied from several seconds to a minute or two. (100 nm diameter was the smallest masking size attempted (Figure 2e).) It is not known whether any polyelectrolyte is transferred from the substrate to the masking particle during its removal. We have no evidence of such transfer, and in any case the contact area is much smaller than the patch size given by eq 1, so that site-specific binding of complementary particles is observed on the patchy surfaces (Figure 2) and particles (Figures 4 and 5).

Figure 2 illustrates surface-charge patterns on the substrate, made manifest by shadowing, fluorescent particle labeling, and direct mass-thickness contrast, as described above. Figure 2b is a combined fluorescence and bright-field optical micrograph, which shows the location of the masking particles (marked by dark Cr evaporation) and of the surface-charge patches (labeled by small bright fluorescent particles). The masking particle here is PS4690s<sup>-</sup>, and the fluorescent label is PS100s<sup>-</sup>. The location of the fluorescent label relative to the positively charged patch is visible by TEM examination (Figure 2c). For this image, the label particle was chosen to be larger for improved contrast. In addition, the blob size in each polyelectrolyte solution can be evaluated using eq 1, i.e.  $d_b \cong r_{\text{patch}}^2/a$ . The patch size was

(40) Yiantsios, S. G.; Karabelas, A. J. *J. Colloid Interface Sci.* **1995**, *176*(1), 74–85.

(41) Verma, R.; Crocker, J. C.; Lubensky, T. C.; Yodh, A. G. *Phys. Rev. Lett.* **1998**, *81*(18), 4004–4007.

(42) Hubbe, M. A. *Colloids Surf.* **1984**, *12*(1–2), 151–178.

(43) Janex, M. L.; Chaplain, V.; Counord, J. L.; Audebert, R. *Colloid Polym. Sci.* **1997**, *275*(4), 352–363.

(39) Denkov, N. D.; Velev, O. D.; Kralchevsky, P. A.; Ivanov, I. B.; Yoshimura, H.; Nagayama, K. *Nature* **1993**, *361*(6407), 26–26.

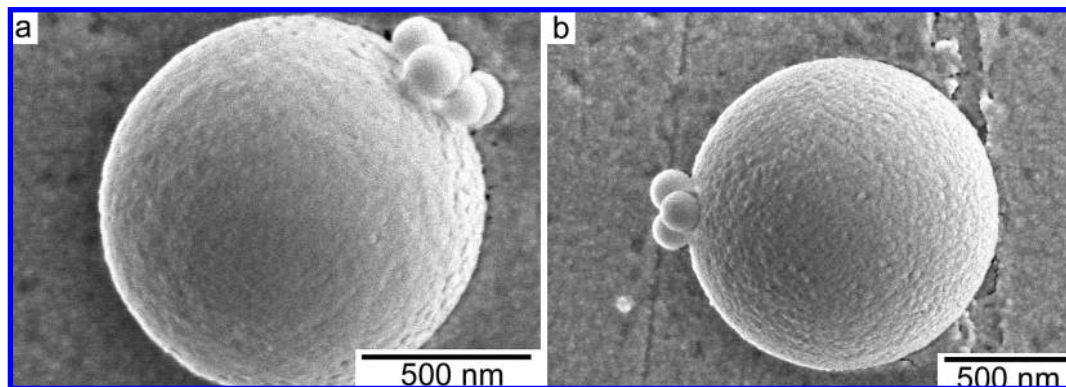


**Figure 5.** SEM images showing PS160c<sup>-</sup> particles attached to the patchy region of PS1100a<sup>+/-</sup> particles.

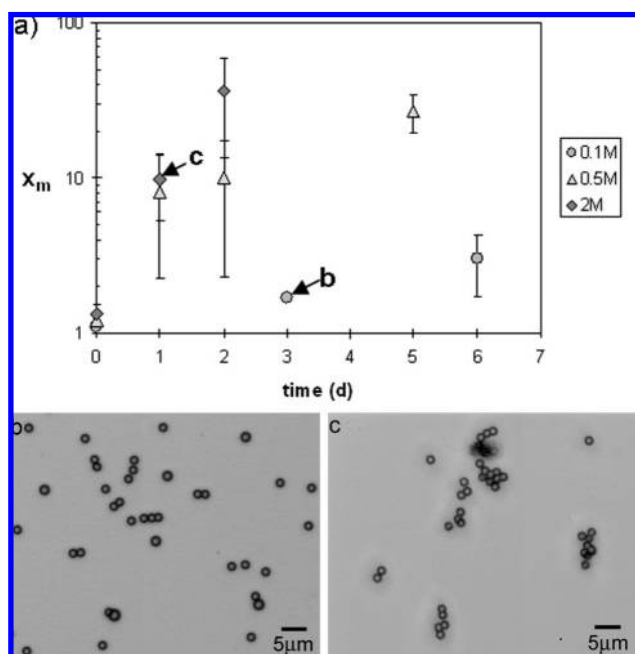


**Figure 6.** Self-aggregation of PS2000c<sup>-/+</sup> patchy particles. (a) Mass-averaged cluster size as a function of time and salt concentration ( $c_s$ ), (M signifies mol/L). Standard uncertainties of the measured distributions are drawn. (b,c) Snapshots of particle distributions: (b)  $c_s = 0.1$  mol/L and 3 days; (c)  $c_s = 2$  mol/L and 1 day.

measured at the inner radius of the thinner (occluded) area (even though some label particles are adsorbed at the outer edge), and the masking particle size was measured by the radius of the Cr shadow. Based on such analysis, the blob size in the PSS solution is  $14 \pm 3$  nm and, similarly, in the PAH solution is  $13 \pm 3$  nm.

These experiments illustrate the yields of both particle lithography and of subsequent binding of particles to the surface patches, which are very high (e.g., Figure 2b, “p”). There are three types of failures: (a) a masking sphere may fail to produce a surface-charge patch (e.g., Figure 2b, “n”), (b) the surface charge patch may remain unlabeled, or (c) the label particles may bind outside of the defined patch (e.g., Figure 2b, “s”). While the stray particles “s” are obvious, distinction between the first two failures is more subtle. In the example “n” in Figure 2b, the shadow in the Cr film overlaps its neighbors, indicating that it was cast from a sphere that was not in contact with the substrate, so that polyelectrolyte was not size excluded there, and no patch can be created on either particle or underlying substrate. TEM mass-thickness observations are consistent, which show no patches under particles with overlapping shadows and do show patches in every case that the Cr shadows are distinct.

Therefore, since these shadows are visible optically, optical microscopy can determine production and labeling yields (Figure 2b). From 10 independent samples of approximately 300 sites each, the failure rate for “n” is approximately  $1\% \pm 1\%$ ; the failure rate of unlabeled sites is approximately  $1\% \pm 1\%$ ; and the fraction of stray particles is approximately  $3\% \pm 1\%$ . While the patch production yield remains high regardless of masking particle size, the labeling yields depend on the sizes of both masking and labeling spheres and on processing conditions. For example, the fraction of labeled sites in Figure 2d is small, even though the surface was bathed with a 2% mass fraction suspension of PS100s<sup>-</sup> for approximately 0.5 h, indicating that longer time or perhaps increased ionic strength may be desirable. The interaction of charged particles with patchy surfaces exhibits interesting subtleties, which depend on the relative sizes of particles, patches, and Debye length, as explored, for example, in recent reports.<sup>44,45</sup>

Next, we consider the rate of production of patchy particles, 300 nm diameter, as an example. This size particle may be adsorbed onto a surface at a density of  $6 \times 10^8$  particles/cm<sup>2</sup>. To review, the process involves coating the substrate with polyelectrolyte, then with particles, again with polyelectrolyte, and removal of particles from the surface by ultrasound. Given a 6 min cycle to complete these steps, the production rate of patchy particles is of the order of  $10^8$  particles/min/cm<sup>2</sup>. A roll-to-roll process can be more efficient. For example, if the speed of the substrate is 0.5 cm/s, a production rate of  $2 \times 10^{10}$  particles/min/(cm substrate width) is feasible. For comparison, 7 mL of 2% mass fraction suspension contains approximately  $10^{13}$  such particles.

These patchy particles are quite stable in suspension at low salt conditions, indicating that their net surface charge is substantial. Measurement of the particle zeta potential confirms that the surface charge has been reversed by application of the polyelectrolyte (Table 1).

**Particle Assemblies.** Patchy particles can potentially form a variety of assemblies in either homogeneous or mixed solutions of particles, and the resultant assembly can be directed through mixing of appropriate particles. Some possible assemblies are illustrated schematically in Figure 3 and experimentally in Figure 4. These experimental mixtures also contain some singlets and a few randomly aggregated particles at 0.3 mol/L NaCl for 1 day. When a solution of patchy particles is mixed with a solution of uniform particles whose surface charge is complementary to the lithographic region, the particles (of different type) bind to

(44) Huang, H. W.; Bhadrachalam, P.; Ray, V.; Koh, S. J. *Appl. Phys. Lett.* **2008**, 93(7), 073110.

(45) Santore, M. M.; Kozlova, N. *Langmuir* **2007**, 23(9), 4782–4791.

each other (Figure 4a and b). These results show the patchy particles exhibit selective aggregation. Self-aggregation also takes place at longer aggregation time (Figure 4c, 2 days). Such aggregation is explored further in a section below. In addition, these results suggest that the lithographic region indeed has the expected surface charge, and therefore, it is not likely to be contaminated by polyelectrolyte that might otherwise have been removed from the substrate during sonication. As a control, patchy particles were also prepared on a bare glass substrate. These also exhibited site-specific binding with complementary uniform spheres in the same way as those patchy particles prepared on an underlying polyelectrolyte film, which as noted above serves to cut dramatically the time required for preparing patchy particles and increase the yield.

In the formation of these doublets, the particle attached to the lithographic patch is larger than the estimated patch diameter. The patch size, however, can be evaluated if the patchy particle is reacted with substantially smaller ones (Figure 5), so that they mark out the lithographic region. For example, PS160c<sup>-</sup> particles were added in excess to patchy PS1100a<sup>+</sup> particles, so that most of the lithographic areas should be fully decorated. According to eq 1, the patch diameter is calculated to be approximately 180 nm. It was found that between one and five (and mainly two and three) 160 nm PS- particles attached (Figure 5), suggesting that the lithographic region is roughly 200–300 nm in diameter, somewhat larger than expected. Likewise, Figure 2 shows particles bound near to (and sometimes over) the edge of the patch. Surface labeling to mark out the lithographic region is a practical yet indirect means of chemical analysis of the patchy particle surface. Unfortunately, elemental analysis of these patchy surfaces is not feasible. For example, Auger microscopy which has excellent surface sensitivity and lateral resolution is not possible here, since the particles are nonconductive and sample charging prevents analysis.

Self-aggregation of patchy particles was observed at only long preparation times or high salt concentration (Figure 6). For example, measurable kinetics of self-aggregation of PS2000c<sup>-</sup> was observed when the salt concentration was at least 0.1 mol/L. At this concentration, the Debye length is approximately 1 nm, that is, much smaller than either the patch or the particle diameter. As the salt concentration is increased, kinetics become faster, as expected. The aggregates exhibit no special structure reflecting the anisotropy of the particles. We suppose that this result occurs, since the size of the patch relative to the whole particle surface is only a few percent. In that case, pairing between positively and negatively charged surfaces can occur in many different

orientations. Self-aggregation that reflects the dipolar symmetry more strongly might be obtained when the patch and the Debye length are relatively large. Such conditions are also likely to accelerate self-aggregation.<sup>46–48</sup>

Particle lithography produces a relatively small patch on spherical particles. However, the processes discussed here seem suitable also for anisometric particles on which the resulting patch would be a substantially larger fraction of the surface.

## Conclusion

The surface charge of polystyrene particles is modified by adsorption of polyelectrolyte to their surfaces. When the particles are in suspension, their entire surface is coated, but if these particles are adsorbed first to a surface, a circular region of the surface is inaccessible, and a patchy particle or surface is produced.

The substrate surface charge has a significant effect on the adsorption of particles, which provided several advantages in comparison to bare glass substrates. These include much reduced deposition time, a high degree of coverage, and the ability to accommodate both negatively and positively charged particles. Moreover, patch production yield is consistently 99% ± 1%. This strategy for depositing polystyrene particles onto a polyelectrolyte film may be compatible with roll-to-roll processing, providing a suitable route to producing large numbers of particles. Considering 300 nm particles, 10<sup>8</sup> particles/min/cm<sup>2</sup> can be produced in batch, or approximately 2 × 10<sup>10</sup> particles/min/(cm roll width) in continuous roll processing.

Particle aggregation and assembly were also investigated. High-yield site-specific binding of complementary spheres to the lithographic region of patchy particles was demonstrated, including binding to positive and negative patches. When the complementary particles are small, they serve well to detect the location of a patch and to measure its size. Since the net charge of these patchy particles is substantial, self-aggregation between patchy particles was observed only at high ionic strength and did not yield unusual structure.

**Acknowledgment.** The authors thank Prof. Andreas Stein for generously donating 600 nm polystyrene particles.

LA8017375

(46) Russel, W. B.; Saville, D. A.; Schowalter, W. R. *Colloidal Dispersions*; Cambridge University Press: New York, 1989.

(47) Yake, A. M.; Panella, R. A.; Snyder, C. E.; Velegol, D. *Langmuir* **2006**, *22*, 9135–9141.

(48) Holtzer, G. L.; Velegol, D. *Langmuir* **2005**, *21*, 10074–10081.